Bioprocess Engineering 1 (1986) 29–41

Bioprocess Engineering

Hydrodynamic effects on cells in agitated tissue culture reactors

R. S. Cherry and **E. T. Papoutsakis,** Houston

Abstract. Tissue cells are known to be sensitive to mechanical stresses imposed on them by agitation in bioreactors. The amount of agitation provided in a microcarrier or suspension bioreactor should be only enough to provide an effective homogeneity. Three distinct flow regions can be identified in the reactor: bulk turbulent flow, bulk laminar flow, and boundary-layer flows. Possible mechanisms of cell damage are examined by analyzing the motion of microcarriers or free cells relative to the surrounding fluid, to each other, and to moving or stationary solid surfaces. The primary mechanisms of cell damage appear to result from (a) direct interaction between microcarriers and turbulent eddies, (b) collisions between microcarriers in turbulent flow, and (c) collisions against the impeller or other stationary surfaces. If the smallest eddies of turbulent flow are of the same size as the microcarrier beads, they may cause high shear stresses on the cells. Eddies the size of the average interbead spacing may cause bead-bead collisions which damage cells. The severity of the collisions increases when the eddies are also of the same size as the beads. Bead size and the interbead distance are virtually equal in typical microcarrier suspensions. Impeller collisions occur when the beads cannot avoid the impeller leading edge as it advances through the liquid. The implications of the results of this analysis on the design and operation of tissue culture bioreactors are also discussed.

List of symbols

d	cm	particle diameter
d_i	cm	impeller diameter
d_s	cm	average surface-to-surface spacing between particles
E_c	g cm^2 s^{-2}	energy of particle-to-particle collisions
$E_{c,i}$	g cm^2 s^{-2}	energy of particle to impeller collisions
g	980 cm s^{-2}	gravitational constant
k	cm^{-1}	surface to volume ratio term, Eq. (10)
l_e	cm	eddy size
m	g	particle mass
n	s^{-1}	impeller rotational speed
n_b	cm^{-3}	number of particles per unit volume
n_B		number of impeller blades
N_c	cm^{-3} s^{-1}	particle-particle collision frequency per unit volume
$N_{c,i}$	cm^{-3} s^{-1}	frequency of particle to impeller collisions per unit volume
N_P		power number
Re		Reynolds number
P	g cm s^{-1}	agitator power consumption
r	cm	radial distance in spherical coordinate system
R	cm	particle radius
R_i	cm	impeller leading edge radius
S_v	cm^{-1}	surface area of beads per unit volume
SC	g cm^{-1} s^{-3}	severity of particle-to-particle collisions per unit volume
SC_i	g cm^{-1} s^{-3}	severity of particle to impeller collisions
t	s	time between particle collisions
$v_{b,r}$	cm s^{-1}	root mean square relative velocity between neighboring particles
v_e	cm s^{-1}	velocity of the smallest eddies
v_f	cm s^{-1}	fluid velocity
v_t	cm s^{-1}	bead terminal velocity
v_ϕ	cm s^{-1}	ϕ component of fluid velocity around a spherical particle
v_∞	cm s^{-1}	fluid approach velocity
V	cm^3	reactor liquid volume
$V_{b,\mathrm{tot}}$	cm^3	total bead volume in reactor
w	cm	impeller blade width
x	cm	distance from impeller leading edge
y	cm	distance from impeller surface
α		volume fraction occupied by particles
β	g cm^{-1} s^{-1}	parameter in shear stress definition
γ	s^{-1}	shear rate
δ	cm	boundary layer thickness
δ_l, δ_t		laminar and turbulent δ, respectively
ε	cm^2 s^{-3}	energy dissipation rate per unit mass
η	cm	size of smallest eddies
θ		angle in spherical coordinate system
μ	g cm^{-1} s^{-1}	viscosity
ν	cm^2 s^{-1}	kinematic viscosity
ϱ_f	g cm^{-3}	fluid density
ϱ_b	g cm^{-3}	particle density
τ	g cm^{-1} s^{-2}	shear stress
$\tau_{w,l}$		wall τ in laminar boundary layer
$\tau_{w,t}$		wall τ in turbulent boundary layer
ϕ		angle in spherical coordinate system
ψ		stream function

Subscripts

avg	average
b	bead
f	fluid
max	maximum

1 Introduction

The ideal bioreactor for tissue culture work is one which is easily controlled while giving rapid and efficient production of the desired product, be it cells, an excreted product, or a molecule that is retained within the cell while it is alive. Maintaining the homeostasis of tissue cells' natural environment is a step towards obtaining this productivity and ease of control. With the use of suspension cell culture reactors, all of the cells in the system can be exposed to the same conditions. These conditions may be held steady or varied with time by the operator, and are not subject to the limitations of diffusion rates and competition for nutrients that are characteristics of hollow fiber or monolith reactors.

Transformed cells and some normal blood cell types will grow in free liquid suspension; most normal cells however are anchorage dependent and must be grown either on the walls of a liquid filled vessel (roller bottles) or on the surface of small polymer beads (microcarriers) which are suspended in the growth medium [1, 2]. These reactors must be stirred to assure homogeneous conditions and to keep the free cells or microcarriers suspended, and this stirring is a source of mechanical stress.

Tissue cells, lacking a cell wall and not being evolutionarily adapted to life exposed to a free-flowing liquid phase, are more sensitive to hydrodynamic forces in their environment than are fungi or bacteria. The particular problem usually cited in tissue culture work is shear from the agitator used to suspend the cells [1–3]. The word shear by itself is ambiguous. A shear stress τ is a force acting on and parallel to a surface and has units of force/area. In a fluid system shear stress is caused by a velocity gradient in a direction perpendicular to the direction of flow. This gradient is called the shear rate γ and has units of velocity/length. The shear stress is related to the shear rate by the formula $\tau = \beta\gamma$, in which β may be a function of τ or γ. For a Newtonian fluid, which is the typical case for cell culture work unless the suspended solids concentration is very high, β is simply the fluid viscosity μ.

Although needed for proper reactor design, quantitative data about shear effects on cells are scarce. Midler and Finn [4] evaluated death rates of 80 μm diameter protozoa in both laminar shear fields and agitated vessels; in the latter system impeller tip speed was the variable that correlated with survival rates. Hirtenstein and Clark [5] showed that increasing stirring speed in a spinner flask causes the growth of Vero cells on microcarriers to pass through a maximum at 60 rpm. Sinskey et al. [6] correlated maximum cell density of chick embryo fibroblasts on microcarriers with an "integrated shear factor" defined as the ratio of impeller tip speed over the distance from the impeller tip to the vessel wall. Wang et al. [7] have reinterpreted that data to show that cell viability drops significantly when the smallest turbulent eddies in the system are of the same size as the microcarriers. Stathopoulos and Hellums [8] report that the viability and morphology of flat monolayers of human embryonic kidney cells are functions of both shear stress and duration of exposure.

Table 1. Representative microcarrier reactor specifications

Liquid		
Volume	V	1 liter
Density	ϱ_f	1.0 g/cm^3
Viscosity	μ	0.007 g cm^{-1} s^{-1}
Microcarrier beads [23]		
Shape		Smooth spheres
Radius	R	75 μm
Density	ϱ_b	1.03 g/cm^3
Concentration		
– dry basis		5 g/liter
– hydrated		7 vol%
Impeller		
Configuration		4 rectangular blades at 45° angle
Diameter	d_i	8 cm
Blade width	w	3 cm
Leading edge radius	R_i	0.1 cm
Rotational speed	n	60 rpm
Tip speed	v	25 cm/s

Shear stress can also affect the rate of production of excreted cell products. Stathopoulos and Hellums [8] describe a maximum in urokinase production by kidney cells at a relatively low applied shear stress (6.5 dyne/cm^2). Frangos et al. [9] discuss increased prostacyclin production by human endothelial cells subjected to a steady shear stress, with even greater production when the shear stress is cyclic with a 1 Hz frequency around the same average value.

Shear has many manifestations within a stirred vessel containing suspended solids, not all of which would be expected to be harmful. In particular, one must distinguish between shear fields caused by the presence of the individual microcarriers and those physically larger fields associated with the reactor walls, agitator and internals. This paper will consider the mechanisms by which hydrodynamic forces can affect cells in agitated cell culture reactors, and specifically microcarrier systems. The magnitude of the various effects will be estimated by repeatedly referring to a standard set of conditions typical of a one liter microcarrier system (Table 1). The effects of bulk liquid turbulence, boundary layers and shear fields, and collisions will each be considered. The results should be useful for rational reactor design and scale-up to any size.

2 Purposes of agitation

Agitation of a cell culture reactor is required to keep the microcarriers from settling out and to assure a homogeneous environment for cell growth. In bacterial fermen-

tations agitation is also used to control the amount of dissolved oxygen by affecting the oxygen transfer rate from the sparged gas into the liquid. In tissue cultures sparging may cause cell lysis and foaming, so other oxygenation systems are often used that diffuse oxygen through a tube or membrane or else oxygenate and recirculate medium from which the cells have been separated [1, 2]. Agitation is not critical to oxygenation with those systems [10], so settling and homogeneity will be considered individually to determine how much agitation is minimally required.

The first item, preventing settling, requires a negligible fluid velocity in the bulk phase. Assuming microcarrier and liquid properties as in Table 1, Stokes' law gives a terminal velocity

$$v_t = \frac{2R^2(\varrho_b - \varrho_f)g}{9\mu} = 0.053 \text{ cm/s},$$

($R = 0.0075$ cm, $\varrho_b = 1.03$ g/cm^3, $\varrho_f = 1.0$ g/cm^3, $g = 980$ cm/s^2, $\mu = 0.007$ g/(cm s)) in which R is the bead radius, ϱ_b and ϱ_f are bead and fluid densities, g is the gravitational constant, and μ is fluid viscosity. The bead Reynolds number is less than one,

$$Re = \frac{\varrho_f v_t 2R}{\mu} = 0.11,$$

so Stokes' law does hold. For free cells such as hybridomas with cell diameter of ca. 20 μm, the settling velocity is only $8 \cdot 10^{-4}$ cm/s, or 2.8 cm/h. With typical flows in a small stirred vessel being turbulent and one to two orders of magnitude larger than the microcarrier settling velocity of 0.05 cm/s, maintaining suspension is not a problem.

At this minimum liquid velocity the Stokes drag force and the buoyant force will balance the force of gravity if the liquid is flowing exactly opposite the direction of gravity. This is true everywhere in a fluidized bed reactor, but in an ordinary stirred tank there are regions of downward and horizontal flow too. These present no problem as long as the beads do not accumulate on the bottom of the reactor. This is prevented by having a curved bottom (such as a hemispherical head) so particles on the bottom are moved horizontally by fluid drag until the vertical component of fluid velocity is sufficient is suspend them. Alternatively, turbulence in the liquid phase can provide instantaneous vertical drag and lift forces sufficient to lift particles off the bottom, regardless of the direction of the mean flows.

We can estimate the maximum shear stress τ_{max} on the microcarrier surface that results from its sinking through the liquid at the settling velocity [11]:

$$\tau_{max} = \frac{3}{2}\frac{\mu v_t}{R} = 0.07 \text{ dyne/cm}^2.$$

This is well below the value of 10 dyne/cm^2 at which significant damage starts to occur to human kidney cells [8]. Settling, or equivalently keeping the cells from settling, does not cause a damaging level of shear stress on the cells.

Maintaining homogeneity by minimizing variations throughout the reactor of dissolved oxygen and other nutrient concentrations or temperature is the primary reason for agitating tissue culture reactors. There will inevitably be local variations, for example higher oxygen concentration near the oxygen source, or slightly different temperatures at the wall of a jacketed reactor. We can approximate the average liquid velocity needed to give effective homogeneity by requiring that the cells move through these areas of different conditions in an amount of time that is small compared to their metabolic response time.

Although there is apparently no data published for tissue cells, Cooney et al. [12] report that pulsed feeding of methanol to Pseudomonas methylotropha gave improved yields when the pulse frequency was greater than once every fifty seconds, and was essentially the same as continuous feeding at a pulse rate of every fifteen seconds. Harrison and Topiwala [13] present data on concentrations of glycolysis intermediates (e.g. glucose-6-phosphate) in Klebsiella aerogenes in response to step changes in oxygen tension, and the time to reach new steady-state values was ten to fifteen seconds depending on the direction of the step change. Hansford and Humphrey [14] give some results for the effect of stirred tank mixing times in the range of 2–3 seconds on the yield of Baker's yeast in a glucose-limited culture at low growth rates. In spite of the limitations of applying data from one species to another, it appears that fluctuations of oxygen and substrate of less than two seconds duration may not cause a significant effect on cell metabolism and growth, particularly if one considers that mammalian cells grow at an order of magnitude lower rate than bacteria or yeasts.

Saying that a one liter cell culture reactor has a characteristic dimension of 10 cm, the minimum liquid velocity needed is on the order of 5 cm/s. This is about one hundred times the settling velocity of the microcarriers, so mixing of the liquid that is sufficient to keep cells from lingering in areas of locally different conditions will be more than enough to keep the microcarriers or free cells from settling under gravity's influence.

In addition, mixing and its associated mechanical stresses may be beneficial in enhancing growth and/or product formation due to the physiological effect of fluid shear stresses [8, 9], as already discussed. In that case, the mixing or agitation of the bioreactor should be designed to provide the spectrum of stresses that gives the optimal cellular response.

3 Bulk liquid turbulence effects

The structure of isotropic turbulence was originally formulated by Kolmogorov in 1941 [15]. The kinetic energy of the velocity fluctuations in turbulent flow is passed

from larger eddies to smaller ones with minimal dissipation until, in the smallest eddies, viscous losses degrade the kinetic energy to heat or in this case possibly to mechanical work in physically damaging cells. Practically, the dissipation of the kinetic energy by the small eddies occurs near or in the viscous sublayers generated by the presence of stationary and moving surfaces, or in the thin shear layers enveloping larger eddies [16].

In assessing the effects on microcarrier-bound or free cells in a flow field, it is the relative motion of the microcarriers or cells through the surrounding fluid that matters rather than the motion relative to the reactor walls. This is, of course, only the case when cell damage originates from fluid mechanical stresses rather than collisions with other particles or solid surfaces. The forces acting on the particle in turbulent flow include

a) drag due to the particle motion relative to the fluid,
b) the net force of gravity and buoyancy,
c) a force from any local pressure gradient,
d) inertial and Magnus forces due to particle rotation, and
e) viscous shear-rate forces [16].

The liquid flow in a typical stirred reactor is at least locally turbulent because of the high impeller tip speed and the various probes, thermowells and sampling tubes that act as baffles. If the scale of the smallest turbulence is sufficiently larger than the microcarriers, the beads just follow the local flow pattern (Fig. 1 a) and move at the local liquid velocity [16]. The microcarriers, being slightly denser than the medium, have a slight inertia which interferes with their tendency to follow the fluid motion. However, for this system, the mean velocity difference is less than 0.1% of the fluid velocity for eddies substantially larger than the beads [17]. The beads still settle at their terminal velocity relative to the liquid in the turbulent eddies, but otherwise do not sense them except for intermittent brief periods of acceleration when they enter a new eddy. As has been shown, the settling velocity alone does not create a damaging level of shear.

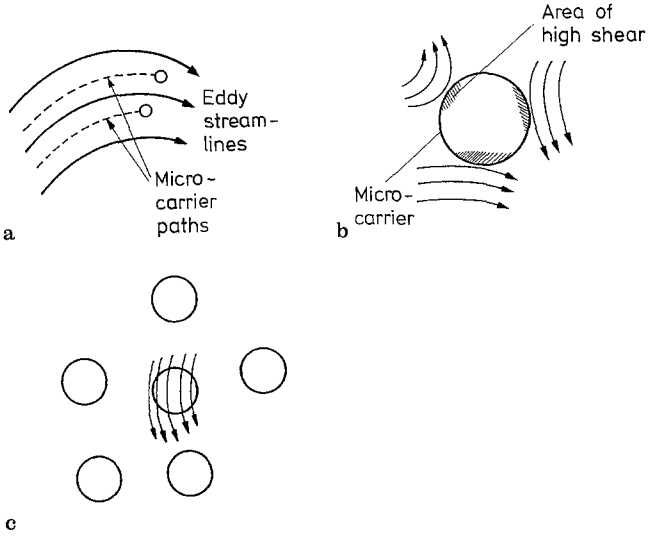

Fig. 1 a – c. Bead-eddy interactions. **a** Eddies much larger than beads. **b** Multiple eddies same size as bead. **c** Eddy size same as interbead spacing

Turbulent eddies of the same size as a microcarrier however may affect cell performance in several possible ways. A single eddy cannot engulf the bead and can only act on part of the surface, causing the bead to rotate. From Kolmogorov's theory [15, 18, 19] the size and the velocity of those smallest eddies are of the order of η and v_e, respectively:

$$\eta = \left(\frac{\nu^3}{\varepsilon}\right)^{1/4} \quad \text{and} \tag{1}$$

$$v_e = (\varepsilon\,\nu)^{1/4}, \tag{2}$$

where ε is the local energy dissipation rate per unit mass of liquid and ν the fluid kinematic viscosity. Solving for v_e as a function of η, which is set numerically equal to the microcarrier diameter,

$$v_e = \frac{\nu}{\eta} = 0.5 \text{ cm/s} \tag{3}$$

($\nu = 0.007\,\text{cm}^2/\text{s}$, $\eta = 0.015$ cm), so eddies the size of a microcarrier have a typical velocity of about 0.5 cm/s. This velocity applied to a point on the surface of a 150 µm bead causes it to rotate at about 10 revolutions per second, which could cause a cell on the bead surface to see a 10 Hz shear variation depending on the conditions all around the bead. Frangos et al. [9] found a 1 Hz shear variation to have a significant positive effect on prostacyclin production. The general effects on cells of this higher frequency are unknown. However, in one case [20] fibroblasts gave up to a 30 times increase in specific interferon production when grown on microcarriers in spinner bottles versus on the walls of roller bottles under identical conditions, although no explanation for the increase was offered.

Alternatively, several eddies the size of the microcarrier could interact with it simultaneously. If their interactions are in the same rotational sense, the bead rotates as just described. If their actions are opposed, the eddies cause a greater shear stress against the part of the microcarrier nearest them (Fig. 1 b) since the bead cannot rotate to cancel each of the shear forces on it. These shear forces are impossible to estimate given the possible ranges of bead-eddy orientations and the transient nature of the interaction.

Eddies significantly smaller than the microcarrier also cause a shear stress if present, but this is best modelled using a turbulent drag coefficient [21]. Their major effect will be on the degree of coupling between bead motion and large-scale eddy flows [16]. However, eddies smaller than the microcarriers would not normally be seen with mixing as mild as is typical of cell culture reactors. This

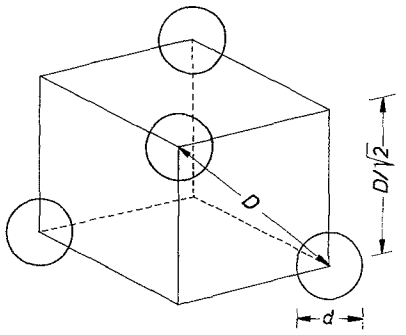

Fig. 2. Microcarrier spacing in suspension

range of effects of eddy sizes much larger than, equivalent to and smaller than the particle size has been used successfully to explain and model particle diffusion in turbulent flows [22].

Turbulent eddies of the same size scale as the microcarrier separation may also cause cell damage by promoting bead-bead collisions. At a typical bead concentration of 5 g dry weight/liter the beads occupy about 7 volume percent after hydration, using a swelling factor of 14 ml/g dry weight [23]. Assuming a tetrahedral arrangement of the microcarriers (Fig. 2) for the sake of these calculations, each space-packing cube of volume $V_{\text{cube}} = (D/2^{1/2})^3$ contains 4 eighth sections of beads with total volume

$$V_{b,\text{tot}} = 4 \cdot \left(\frac{1}{8}\right) \cdot \left(\frac{4\pi (d/2)^3}{3}\right) = \frac{\pi d^3}{12}.$$

Knowing the volume fraction of beads is 0.07,

$$0.07 = \frac{V_{b,\text{tot}}}{V_{\text{cube}}} = \frac{\pi d^3}{12 (D \cdot 2^{1/2})^3} = \frac{\pi 2^{1/2} d^3}{6 D^3}$$

from which,

$$\frac{D}{d} \simeq 2.2 .$$

Since D, the center-to-center bead spacing, includes the radii of two beads, the surface-to-surface spacing is

$$d_s = 2.2 d - 2\left(\frac{d}{2}\right) = 1.2 d , \tag{4}$$

which is nearly equal to the bead diameter.

Eddies much larger than the bead spacing can move groups of beads without causing large relative velocities between them. Einav and Lee [24] found that in laminar flow (corresponding to the limiting case of infinite eddy size) suspensions of 4–6 vol% neutrally buoyant 100 μm spheres had essentially no bead-bead collisions. It is easily conceivable that eddies the size of the interbead spacing could accelerate one bead without disturbing another nearby (Fig. 1c). The two beads then have a significant relative velocity and a finite chance of collision.

Hinze [16] has estimated the turbulent collision frequency for low concentrations of suspended solids (< 0.1 vol%). Higher concentrations may alter the structure of turbulence because of inter-particle fluid shear, wakes produced by moving particles, the reduced total liquid volume and group movement of particles. Because microcarriers have roughly the same density as the medium and so will behave energetically like packets of medium, and because the particle and interparticle dimensions are of the same or smaller order of magnitude as the scale of the smallest turbulence, the effect on the general turbulent structure should not be excessive. We shall use Hinze's result [16] to see the effect on collision frequency of some important bioreactor parameters.

The collision frequency per unit volume N_c is of the order

$$N_c \sim \left(\frac{v_{b,r}\, \alpha^2}{d^4}\right), \tag{5}$$

where $v_{b,r}$ is the root mean square relative velocity between neighboring particles. If the size of eddies l_e is much larger than the particle size d, particles move in groups with very small or zero $v_{b,r}$, except for very short time periods when fluid is exchanged between eddies (see Fig. 1a). This is independent of the average distance between particles (or, equivalently, α). However, $v_{b,r}$ becomes significant and eventually large as the eddy size becomes comparable to or smaller than the size of either the particles d or the average distance between particles d_s ($d \le d_s$). For eddy sizes smaller than or comparable to d_s, eddies can engulf no more than one particle (if $l_e > d$) and can thus generate relatively large $v_{b,r}$ values even for large particles. If l_e is of the same order of magnitude as d, $v_{b,r}$ can attain even larger values, because smaller eddies attain larger velocities (Eq. (3)). In either case, $v_{b,r}$ is of the order of the eddy velocity. Since, as we have already discussed, the size of the smallest eddies η (Eq. (1)) is most unlikely to be smaller than d, we shall take $v_{b,r}$ to be of the order of the velocity v_e (Eq. (2)). Thus:

$$N_c \sim \left(\frac{(\varepsilon \nu)^{1/4} \alpha^2}{d^4}\right). \tag{6}$$

As expected, increased agitation energy input (larger ε) causes more collisions, as does an increased concentration α of beads.

The velocity may also be expressed in terms of eddy size η (Eq. (3)) to give

$$N_c \sim \left(\frac{\nu \alpha^2}{\eta\, d^4}\right). \tag{7}$$

The variables α, η, and d are not all independent. The volume fraction α is set by the desired surface area S_v of beads per volume of suspension (which determines the ultimate cell density):

$$S_v = n_b \pi d^2 , \tag{8}$$

where n_b is the number of beads per volume of suspension. Since, $n_b = \alpha / V_b$ (where V_b is the individual bead volume) we obtain

$$S_v = \frac{6\alpha}{d} \tag{9}$$

and hence

$$\alpha = \frac{S_v d}{6} \equiv k\, d\,, \tag{10}$$

in which $k = S_v/6$ is determined by the desired cell density in the system and is essentially independent of the bioreactor configuration. Furthermore, assuming that the inter-bead spacing is approximately equal to η (Eq. (4)),

$$\alpha \simeq \left(\frac{d}{d+\eta}\right)^3 \simeq k\, d\,,$$

$$\eta \simeq \left(\frac{d^2}{k}\right)^{1/3} - d\,. \tag{11}$$

From Eqs. (7), (10) and (11) we then obtain,

$$N_c \sim \left(\frac{\nu\, k^{7/3}}{d^{8/3}\,(1-(k\,d)^{1/3})}\right). \tag{12}$$

The bracketed term in the denominator is of order one, so

$$N_c \sim \left(\frac{\nu\, k^{7/3}}{d^{8/3}}\right). \tag{13}$$

Thus, the collision frequency is strongly dependent on the particle diameter when the smallest eddies are the size of the bead spacing. For typical conditions, $k = 2.4\ \mathrm{cm}^{-1}$ and $N_c \sim 4{,}000$ collisions/(s cm^3), or roughly one collision per bead every five seconds.

The severity of collisions SC, defined as the energy E_c times the frequency N_c of collision, will be of the order of

$$SC \sim ((m\, v_{b,r}^2)\, N_c)\,,$$

because E_c is of the order of $m\, v_{b,r}^2$ or $\varrho_b\, \pi\, d^3 v_{b,r}^2/6$. Since $v_{b,r}$ was taken of the order of v_e, and η of the order of d, we obtain

$$SC \sim \left(\frac{\varrho_b\, \pi\, (\varepsilon\, \nu)^{3/4}\, \alpha^2}{6\, d}\right) \tag{14a}$$

or

$$SC \sim \left(\frac{\varrho_b\, \pi\, \nu^3\, k^{7/3}}{6\, d^{5/3}}\right). \tag{14b}$$

The effect of d on the severity of collision may be hard to generalize because smaller beads are expected to result in more collisions of lower energy each. In any case, the cellular responses to frequency and energy are unlikely to be linear – if a certain blow kills the cell, hitting it twice as hard does not make it twice as dead – so the net effect is uncertain. It should conceivably be in either direction depending on the relative sensitivity to and the magnitude of frequency and energy terms.

We should emphasize that Eqs. (6), (7), and (11)–(14) are only valid if the size of the smallest eddies η is of the order of the bead size d and inter-bead spacing d_s. For $\eta \gg d$ and $\eta \gg d_s$, N_c, E_c and SC decrease dramatically and would be expected to go to zero for $d/\eta \to 0$ and $d_s/\eta \to 0$. Thus, the expressions for all three N_c, E_c, and SC should be multiplied by a factor which goes to 1 for d/η and d_s/η of the order of 1, and goes to 0 for d/η and d_s/η going to 0. Empirically, neither of these ratios has values much greater than one because eddy sizes less than d_s or d are not typical.

The collisions between beads can have a variety of effects on the cells covering the beads. A head-on collision flattens the cells at the point of collision, possibly rupturing them depending on the energy of collision and the elasticity of the cells. As the collision becomes more and more off-center, the cells in contact between the two beads see less compression but a larger component of shear force, which will in turn depend on the coefficient of friction of two cells sliding over one another. In the limiting case of a slight touch as one bead passes another, the cells feel only a shear force. The gross effect of this may be either cell rupture or detachment from the bead surface. The physiological effects of nonfatal compression or mechanical shearing are not known. The analysis of collision is further complicated by any rotation the beads might have, which would in general contribute an additional shearing component to the force of the collision.

Past empirical efforts to improve cell culture reactors have centered on reducing "shear". The result has been reduced turbulence, hence lower local energy dissipation ε, and an increase in the size of the smallest eddies. For stirred tanks ε is a function of the local liquid flow pattern, and is highest near impeller tips, baffles, and where two opposing fluid streams contact each other [19]. Local values can be calculated directly from measurements of the instantaneous fluid velocity, or an average value can be estimated for the vessel from the measured power input by the agitator motor, although the latter method is better suited to non-baffled reactors in which the fluid turbulence is more uniform throughout.

An average value may also be calculated if the impeller geometry and operating conditions are known. There exist relationships (Fig. 3) that relate dimensionless power consumption N_P to impeller Reynolds number Re and ε:

$$Re = \frac{d_i^2\, n\, \varrho_f}{\mu}\,, \tag{15}$$

$$N_P = \frac{P\, g}{\varrho_f\, n^3\, d_i^5}\,, \tag{16}$$

$$\varepsilon = \frac{P\, g}{\varrho_f\, V} = \frac{N_P\, n^3\, d_i^5}{V}\,. \tag{17}$$

where P is power consumption by the impeller, n is impeller speed in revolutions per unit time, d_i is impeller

Table 2. Smallest eddies calculated for various impeller speeds and blade angles

	20 rpm			60 rpm			100 rpm		
	30°	45°	90°	30°	45°	90°	30°	45°	90°
$Re = \left(\frac{d_i^2 n \varrho_f}{\mu}\right)^*$	2,300	2,300	2,300	7,000	7,000	7,000	11,500	11,500	11,500
$N_P = \left(\frac{P g_c}{\varrho_f n^3 d^5}\right)^{**}$	0.4	0.6	0.9	0.3	0.5	0.7	0.25	0.4	0.6
$\varepsilon = \left(\frac{N_P n^3 d^5}{V}\right)$	0.49	0.73	1.09	9.8	16	23	38	61	91
Eddy size $l_e = \left(\frac{\nu^{3/4}}{\varepsilon^{1/4}}\right)$	0.029	0.026	0.024	0.014	0.012	0.011	0.0010	0.009	0.008

* Using typical conditions from text
** From Figure 3

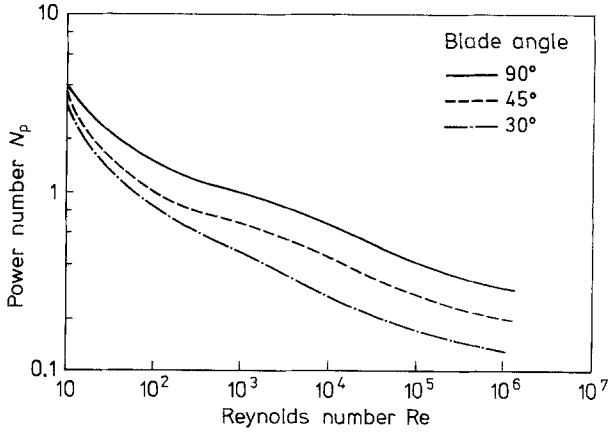

Fig. 3. Power number correlation for two-bladed impeller at various blade angles. Adapted from Nagata, Fig. 1.21 [19]

diameter, and V is the agitated liquid volume [25]. In these macroscopic relations the fluid viscosity used should account for the effect of suspended solids. The expected increase is about 30% over the clean fluid value for 7 vol% solids [26, 27]. With these expressions it is possible to determine the scale of the smallest turbulence from directly measurable reactor parameters. Using typical values ($d_i = 8$ cm, $n = 1\ s^{-1}$, $\varrho_f = 1$ g/cm^3 and $\mu = 0.007$ g/(cm s)),

$$Re = \frac{d_i^2 n \varrho_f}{\mu} = 7{,}000\,.$$

Referring to Fig. 3, for an unbaffled vessel with a 45° blade angle and 60 rpm rotation, $Re = 7{,}000$ gives $N_P \approx 0.5$ hence $\varepsilon = 16$ cm^2/s^3. This gives a size for the smallest turbulent eddies of

$$\eta = \left(\frac{\nu^3}{\varepsilon}\right)^{1/4} = 0.012 \text{ cm}$$

($\nu = 0.007$ cm^2/s, $\varepsilon = 16$ cm^2/s^3), which compares with a microcarrier diameter of 0.015 cm and a typical bead spacing of 0.018 cm. In this calculation the viscosity effect of solids is not included because the solids are of the size scale as the fluid eddies and do not affect the eddies' internal viscosity.

Table 2 shows similar calculations for 30, 45 and 90° paddle impellers at 20, 60, and 100 rpm. Angling the blades from 90° to 30° causes about a 25% increase in eddy size on the basis of these calculations. In practice the vortices generated by the 90° blades may cause much higher local power dissipation near the impeller than angled blades even though the total power input is similar, so the actual benefit may be more than this indicates. For 90° blades the ratio of power dissipation rate at the impeller to that averaged over the whole vessel is 5.2 and is independent of impeller speed for impeller Reynolds number between 8,000 and 120,000 and impeller diameters half the vessel diameter [28]. The scale of the impeller local turbulence is then $(5.2)^{-1/4} = 0.66$ the scale of the vessel turbulence.

To see the importance of other reactor variables, the N_P expression for ε (Eq. (17)) is substituted into the expression for eddy size η (Eq. (1)):

$$\eta = \left(\frac{\nu^3 V}{N_P n^3 d_i^5}\right)^{1/4}. \tag{18}$$

Reactor volume V is fixed by production requirements. N_P varies in a relatively narrow range for reasonable values of N_{Re} so the 1/4 power of it is ineffectual in significantly changing eddy size, as seen in the blade angle discussion. The important factors to change eddy size are $\nu^{3/4}$, $n^{-3/4}$ and $d_i^{-5/4}$.

In summary then, cells on beads are most affected by turbulence of a size scale the same as the average bead spacing or smaller (causing collisions) or the bead diameter (causing rotation or high local shear on the bead sur-

face). In a typical one liter reactor these dimensions are effectively the same, emphasizing the empirical significance of this eddy size. The turbulent eddies may be made larger, and cell damage presumably reduced, by increasing kinematic viscosity or reducing impeller diameter and speed. If the eddy size can not be sufficiently increased, using a larger bead diameter may reduce the collision frequency, and may, depending on the behavior of the cells, improve the performance of the bioreactor.

4 Boundary layer shear forces

Relatively large areas of high shear rate are expected in the boundary layers around the solid objects submerged in the reactor. The moving impeller would be expected to have the highest velocity relative to the liquid, so we shall analyze it in detail to characterize the general effect of boundary layer shear forces on microcarriers. Much of this discussion can also be applied to the hydrodynamically similar case of the physically much larger shear fields expected in a non-turbulent, laminar flow reactor.

As a first approximation marine and angled flat impeller blades can be modelled as stationary flat plates with fluid moving over them. Einav and Lee [14] have shown that 4 and 6 vol% suspensions of neutrally buoyant spheres do not change the boundary layer shape or development from that predicted for "clean" fluids. The Reynolds number for transition from laminar to turbulent flow over a flat plate is about $3 \cdot 10^5$ [29]. For a typical impeller

$$Re_{\text{plate}} = \frac{\varrho_f v w}{\mu} \simeq 11{,}000$$

($\varrho_f = 1.0$ g/cm^3, $v = 25$ cm/s, $w = 3$ cm, $\mu = 0.007$ g/(cm s)), where v is the velocity of the fluid over the blade and w is the width of the impeller blade in the direction of fluid flow. A laminar boundary layer is expected. However, Schlichting [30] reports that impeller rotation can considerably reduce the Reynolds number for transition. Because of this, the turbulent flow around the impeller, and the possibility of boundary layer separation from the angled blades, both laminar and turbulent boundary layers will be considered.

In the laminar case the boundary layer thickness δ_l [31], defined as the distance from the impeller surface at which the fluid velocity reaches 99% of the free fluid velocity v_∞, is

$$\delta_l \simeq 5 \left(\frac{\nu x}{v_\infty}\right)^{1/2}, \tag{19}$$

where x is the distance from the leading edge of the impeller, neglecting "entrance effects" at the leading edge. For our example

$$\delta_l \simeq 0.084\, x^{1/2}\ \text{cm}. \tag{20}$$

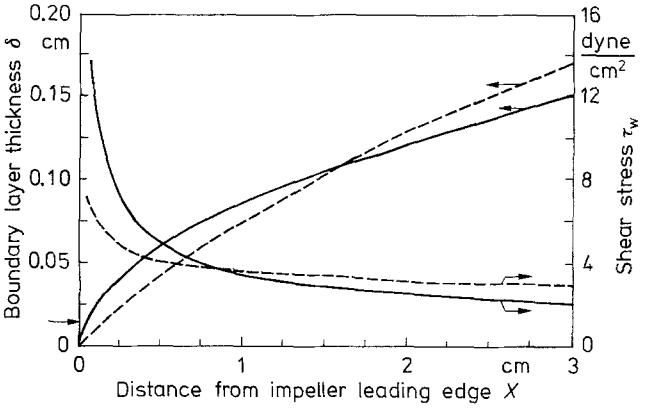

Fig. 4. Boundary layer thickness and wall shear stress on the impeller. —— laminar, ---- turbulent. Arrow indicates microcarrier diameter

The boundary layer becomes as thick as the diameter of a microcarrier ($\delta = 0.015$ cm) at ~ 0.03 cm from the leading edge (Fig. 4). If we arbitrarily say that the boundary layer must be at least three times the microcarrier diameter not to be completely disrupted by the presence of a bead, the corresponding distance is ~ 0.3 cm from the leading edge. At the trailing edge of the 3 cm wide blade the boundary layer thickness is 0.15 cm, or about 10 bead diameters.

Within this boundary layer the highest shear stress occurs at the solid surface. This wall shear stress is calculated from the formula

$$\tau_{w,l} = (0.332)\, \mu\, v_\infty \left(\frac{v_\infty}{\nu x}\right)^{1/2} = 3.47\, x^{-1/2}\ \text{dyne/cm}^2, \tag{21}$$

in which 0.332 is the slope of the dimensionless velocity profile at the wall [31]. At the point where the boundary layer is three bead diameters thick the shear stress is 6.4 dyne/cm^2. Over the remainder of the blade the wall shear stress gradually decreases. The wall shear would be important in systems such as roller bottles in which the cells are attached to the walls. Although wall shear stress itself cannot harm the cells on a suspended microcarrier, this value is reported because the references to shear stress effects are not clear as to what stress is important, and some imply a wall shear stress [6]. This value could also be correlated to shear rates within the boundary layer.

For turbulent boundary layers the formulas for boundary layer thickness and wall shear stress are [29]

$$\delta_t = 0.37\,(x) \left(\frac{v_\infty x}{\nu}\right)^{-1/5} = 0.072\, x^{4/5}\ \text{cm} \tag{22}$$

and

$$\tau_{w,t} = 0.0128\, \varrho_f v_\infty^2 \left(\frac{v_\infty (7/72\, \delta_t)}{\nu}\right)^{-1/4}. \tag{23}$$

Substituting the expression for δ_t (Eq. (22)),

$$\tau_{w,t} = 0.0294\, \varrho_f v_\infty^2 \left(\frac{v_\infty x}{\nu}\right)^{-1/5} = 3.6\, x^{-1/5}\ \text{dyne/cm}^2. \tag{24}$$

Table 3. Boundary layer forces

Force	Resultant bead motion relative to surface
Fluid drag	Parallel, normal and/or rotational
Gravity and buoyancy	Normal
Effect of pressure gradients [a]	Parallel, and/or normal
Saffman lift force [33]	Normal
Added mass effect [b] [16]	Parallel
Bassett force [b] [16]	Parallel
Magnus force [b] [33]	Normal

[a] Important only in turbulent boundary layers
[b] Not important in this system

Values for these functions are compared to their laminar equivalents in Fig. 4. Up to 0.3 cm from the impeller leading edge the two sets of results are significantly different, but this is also the area where the flat plate assumption of the calculations is least valid and the presence of a microcarrier bead causes the greatest disruption to the boundary layer. Past 0.5 cm, and over the majority of the blade, the results are similar: there is a boundary layer of 0.1 cm thickness ($\simeq 7$ bead diameters) with a relatively low shear rate within it.

Within the boundary layer a number of effects may occur (Table 3). Considering the simpler case of a laminar boundary layer, the bead will certainly try to follow the fluid motion which has components both parallel to and perpendicular to the blade surface. Particle motion parallel to the blade is a combined result of the particle's initial velocity and fluid drag. There is also an effect due to the presence of the solid impeller surface that slows the particle's motion [32]. This retardation is particularly important when the bead is within one radius of the surface. There are two other parallel forces [16], the Bassett force, which arises from the work necessary to establish a new fluid flow pattern when the bead is accelerated rapidly, and the added mass effect, which accounts for the behavior of the displaced fluid. These terms are negligible over most of the impeller, and are of consequence only at the leading edge.

The fluid velocity which causes the drag force normal to the impeller is a consequence of boundary layer development in an incompressible fluid and is directed away from the impeller. On the upper surface of the blade, gravity opposes the drag force of this normal flow. As with parallel motion, near the wall the hydrodynamic effect on the fixed surface damps any vertical motion.

There is also a lift force derived from the velocity gradient in the boundary layer [33]. This Saffman lift force is present only when the bead has a slip velocity relative to the fluid streamline that would pass through the sphere's center. It acts to move the bead towards the streamlines which most oppose the slip velocity, so for example a bead moving faster than the local fluid tends to move down the velocity gradient. Near the impeller leading edge the bead will move over the impeller surface faster than the fluid because of its initial inertia, and the lift force will be toward the blade. Further back on the blade fluid drag will slow the bead and the effect of the nearby surface causes the bead to lag the fluid motion. This lag has been demonstrated by Einav and Lee [24], and the resulting lift force is away from the impeller. There is another lift force acting from the Magnus effect on a sphere rotating in a constant velocity field. This force is superimposed on the Saffman force in this system. However, Saffman [33] has shown that the Magnus force is negligible compared to the lift caused by the shear field.

Immich [34] has analyzed these effects for impulsive motion of an infinite plate. While his system is not exactly analogous since it has no normal velocity caused by boundary layer development (since $\partial v_x/\partial x = -\partial v_y/\partial y = 0$), he does give both short and long time solutions for fluid and particle velocities in the parallel and normal directions, particle rotation, and particle concentration.

The shear field in the boundary layer also causes the bead to rotate [35, 36]. In Couette flow (a linear velocity gradient) the angular velocity ω (radian/s) of the sphere will be one-half the fluid shear rate γ_f, but as the bead comes within one-half diameter of the surface, ω slowly decreases because of hydrodynamic interaction with the wall [37]. Unlike in Couette flow, in a boundary layer the shear rate is not constant either in space or time as the particle moves, so these results must be applied with caution. Similarly, experimental data using spheres in tubes [38] are not directly applicable since the spheres are often large compared to the tube radius, and the effect of curvature of the flow field in the tangential direction (perpendicular to both the axis and radius) has not been reported. Nonetheless, assuming that Couette flow results apply, for the system of Table 1 and Fig. 4 a rotational rate on the order of 20 revolutions per second is predicted, similar to the 10 Hz predicted for turbulent rotation.

The magnitude of the shear force on the rotating bead in steady state Couette flow may be estimated from equations developed by Cox et al. [35], using the coordinate system of Fig. 5 and evaluating at $\phi = 0$ and $\theta = \pi/2$ where the shear will be maximal. The shear rate γ_b is

$$\gamma_b = \frac{\partial v_\phi}{\partial r} = \frac{\partial}{\partial r}\left((r\sin\theta)\frac{\partial \phi}{\partial t}\right)$$

$$= \frac{\partial}{\partial r}\left((r\sin\theta)\left(\frac{\gamma_f}{2}\left(\frac{\sin^2\phi - \cos^2\phi}{r^5}\right) + \gamma_f \cos^2\phi\right)\right), \qquad (25)$$

$$\gamma_{b,\max} = \gamma_b|_{\phi=0,\,\theta=\pi/2} = \gamma_f\left(1 + \frac{2}{r^5}\right). \qquad (26)$$

The equation in the original paper is not dimensionally consistent as written, apparently because they substituted a value of unity wherever the sphere's radius should

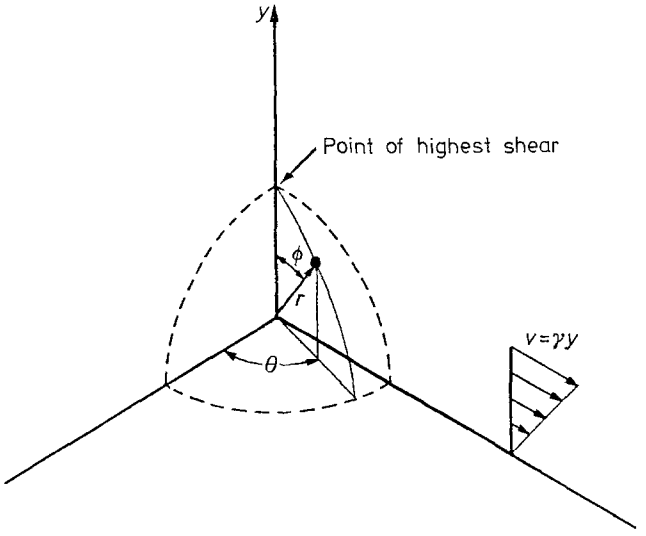

Fig. 5. Coordinate system for a bead in a shear field

appear. Setting $r = 1$ to find the shear rate at the bead's surface,

$$\gamma_{b,\max} = 3\gamma_f, \tag{27}$$

where γ_f is the shear rate in the fluid in the absence of the bead. With 250 s^{-1} as the average shear rate in the 0.1 cm boundary layer of the example system, the maximum shear stress on the bead is of the order $3\mu\gamma_f$ or 5 dyne/cm^2, a nondestructive level [8].

The average shear rate is much lower than the maximum. Integrating over the surface of the bead, using Eq. (25) for γ_b,

$$\gamma_{b,\text{avg}} = \left.\frac{\int_0^{2\pi}\int_0^{\pi} \gamma_b r^2 \sin\theta \, d\theta \, d\phi}{\int_0^{2\pi}\int_0^{\pi} r^2 \sin\theta \, d\theta \, d\phi}\right|_{r=1} = \frac{(2\pi\gamma_f)}{(4\pi)} = \frac{1}{2}\gamma_f. \tag{28}$$

This leads to an average shear stress of $\frac{1}{2}\mu\gamma_f$ or about 0.9 dyne/cm^2 on the bead surface.

Overall, in a laminar boundary layer the microcarrier bead appears well protected from damage. The particle tends to move away from the impeller surface (except perhaps near the leading edge), it rotates at a moderate speed, and the cells on its surface do not see excessive shear stress. There are no bead-bead collisions either [24]. In a turbulent or separated boundary layer the same basic situation holds except for the additional presence of turbulent eddies (discussed under bulk turbulence). These create the possibility of bead impact against the impeller or other beads because of randomly oriented velocity fluctuations occurring in the boundary layer or intruding from the bulk liquid.

5 Collision damage

Cells might also be damaged by a collision of the microcarrier with a solid object, either another microcarrier bead or some part of the reactor. Bead-bead collisions can be caused by changes in liquid direction and velocity over very small distances and were discussed in connection with small scale turbulence. Low velocity collisions may result from a lift force on the bead moving it toward the impeller, gravitational settling or from turbulent velocity fluctuations that propel a bead against the surface.

High velocity collisions with the impeller or other parts of the reactor can occur when the blade advances through the fluid or the fluid flows around a fixed object. Microcarriers flowing on a streamline that passes within one particle radius of the surface will collide with the surface, a process called interception [39]. In addition, the microcarriers, being slightly more dense than the fluid, will not follow the fluid streamlines exactly. Inertia will tend to make the microcarrier travel in a straight line rather than flow around the object with the fluid, increasing the chance of collision. The deviation from the fluid streamline will be most severe where the streamlines are most curved, as is the case at the leading edge of the impeller blade.

Collisions of this sort have been well studied in connection with aerosols and filtration technology [40], but the formulas derived for that work only apply for collector and particle Reynolds numbers much less than one, using collector (impeller) leading edge diameter and particle diameter as the length scales. In the microcarrier system the Reynolds number for the impeller leading edge is 700 and for the particle 55. These are well above the Stokes flow range, but not in the region of fully developed turbulent flow ($Re > 3 \cdot 10^5$ [41]). To estimate collision frequency, we will assume a very high Reynolds number and use equations developed for potential flow [42]. This potential flow assumption is usable because only the extreme leading edge of the impeller is of concern here. Near this stagnation point the boundary layer thickness is constant [43]. If we assume the effect of the stagnation point reaches one leading edge radius R_i upstream, the thickness δ of the boundary layer to where the fluid velocity is 90% of the potential flow velocity is [43]

$$\delta = 1.4\left(\frac{\nu R_i}{v_\infty}\right)^{1/2} = 0.0074 \text{ cm}$$

($\nu = 0.007$ cm^2/s, $R_i = 0.1$ cm, $v_\infty = 25$ cm/s) or about one bead radius. The bead can easily penetrate a layer of this thickness, so we will not consider it further in estimating the collision frequency.

The potential flow pattern around a circular cylinder is used here to approximate the flow around the rounded impeller leading edge (Fig. 6). Other models, such as a flat plate with zero leading edge radius, give results of

similar magnitude. Inertial deviation of the bead trajectory from the streamlines will not be considered. Streamlines are repreented by lines of constant ψ [42], where

$$\psi = v_\infty y\left(1 - \frac{R_i^2}{x^2+y^2}\right). \tag{29}$$

The closest approach of the streamlines to the impeller is at $x = 0$. The microcarrier bead's center must remain at least one bead radius away from the impeller at this point to avoid collision, so on the closest no-collision streamline,

$$x = 0\,, \quad y = R_i + R$$

and

$$\psi = v_\infty (R_i+R)\,\frac{(R_i+R)^2 - R_i^2}{(R_i+R)^2} = v_\infty \frac{2R\,R_i + R^2}{R_i+R}. \tag{30}$$

At a great distance upstream of the impeller along this same streamline, $x \to \infty$ but $\psi = \text{const}$, so we may solve for y_∞:

$$\lim_{x\to\infty} \psi = \lim_{x\to\infty} v_\infty y\left(1 - \frac{R_i^2}{x^2+y^2}\right) = v_\infty y_\infty = v_\infty \frac{2R\,R_i + R^2}{R_i+R}.$$

Therefore:

$$y_\infty = \frac{2R\,R_i + R^2}{R+R_i}. \tag{31}$$

But since typically $R \ll R_i$, y_∞ is approximately $2R$, or equal to the bead diameter d. Any bead vertically within one bead diameter of the streamline passing through the center of the cylinder used as the leading edge model will hit the impeller. Because inertial deviation was not considered, the actual value will be somewhat larger.

Assuming a typical impeller (Table 1) turning at 60 rpm with only the outer half of each blade outside the central cylinder of fluid that rotates with no velocity relative to the impeller [44], to pass the entire reactor contents of 1 liter through this collision window of streamlines takes

$$t_{60\,\text{rpm}} = \frac{\text{Volume of reactor}}{(\text{Area of collision window})\,(\text{Velocity})} = \frac{V}{\left(n_B\left(\frac{1}{2}\right)\left(\frac{d_i}{2}\right)(2d)\right)\left(\pi\frac{3}{4}d_i\,n\right)} = 220\text{ s}. \tag{32}$$

($V = 1{,}000\text{ cm}^3$, $n_B = 4$, $d_i = 8$ cm, $d = 0.0150$ cm, $n = 1\text{ s}^{-1}$, $w = 3$ cm) in which $\frac{1}{2}(d_i/2)$ is the active individual blade length and $\frac{3}{4}d_i$ represents the average diameter of the active section of the impeller blade. On average, each microcarrier hits the impeller once each 220 seconds if the entire reactor is well mixed. This is 1/40 the frequency of bead-bead collisions, but the energy of collision is 2,500 times greater because of the higher relative velocity.

The collision rate is proportional to the agitator speed since inertial effects on the height of the collision window

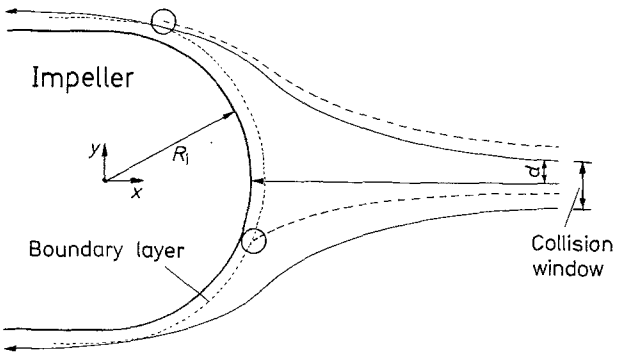

Fig. 6. Streamlines around impeller leading edge. Beads inside the collision window strike the impeller

are not included in this calculation. In addition, the kinetic energy of the collision is much higher, increasing with bead mass and the square of impact velocity which is proportional to agitator tip speed. Combining these effects,

$$SC_i = N_{c,i}E_{c,i} \sim \left(\frac{3\pi\,n_B\,d_i^2\,dn}{8V}\right)\left(\frac{m}{2}\left(\pi\,n\,\frac{3}{4}d_i\right)^2\right) = \left(\frac{9}{512}\pi^4\frac{\varrho_b\,n_B\,n^3\,d_i^4\,d^4}{V}\right). \tag{33}$$

Severity of collisions with the impeller is proportional to the cube of agitator speed and the fourth power of impeller diameter and bead diameter. Since tip speed equals $\pi\,n\,d_i$, note that there is also a third power dependence on tip speed. Because the number of blades appears as only a first order term, there would seem to be a major advantage to using more impeller blades of lesser diameter in order to reduce collision damage. However, as with bead-bead collisions in turbulence, the effect of collision severity (as defined here) on such things as cell viability or maximum cell density is certainly not linear, and may even have a minimum or maximum within the practical range of severity values. Variables such as impeller diameter and rotational speed and bead diameter affect both frequency and energy in the same direction and should show a simpler behavior. Note that this result may explain the apparently greater resistance to "shear forces" of transformed cells, which grow in free suspension, compared to normal cells which must be grown on microcarriers. The diameter difference of free cells and microcarriers is roughly a factor of ten, implying a 10,000 times difference in impeller collision severity. Of course, the smaller size of suspended free cells also protects them from the effects of turbulence because they are much smaller than the smallest eddies as we have already discussed.

The nature of the surface the cell covered bead hits will affect the amount of cell damage that results. A hard surface will concentrate the total collision force on one or

two cells directly in contact with the surface, and will perhaps cause the bead to distort and disrupt cell attachment. An elastic impeller coating softer than the bead could both absorb some of the collision energy and distribute the remainder over a broader area on the bead, reducing the force that individual cells are subjected to.

Smoothness of the impeller surface is important too, to avoid spikes or sharp-edged holes or ruts that could cause damage during what might only have been a glancing impact. Such surface roughness would be significant at the scale of the individual cells' dimension – about 10 μm. Avoiding this potential problem requires a very smooth surface, suggesting that polishing of machined, cast or welded impellers would be of benefit.

6 Implications for reactor design

Two effects stand out as likely causes of cell damage or poor performance in microcarrier tissue culture reactors: turbulence of a size scale comparable to the microcarriers or the spacing between them, and collisions with solid objects, particularly the impeller. The smallest eddies in a turbulent flow are characterized by a length scale $(\nu^3/\varepsilon)^{1/4}$. This size has been increased empirically by reducing ε, the local energy dissipation rate, through such design changes as eliminating baffles, using marine rather than paddle impellers, reducing agitator speed, and using hemispherical rather than flat reactor bottoms. Each of these reduces turbulence, hence ε, in some part in the reactor.

Further advances in increasing the scale of turbulence can be achieved by raising the fluid kinematic viscosity. Because the turbulence scale depends on $\nu^{3/4}$ compared to $\varepsilon^{1/4}$, the effect should be much stronger. To minimize osmotic effects, high molecular weight polymers or gums are good candidates to add to the culture medium. However, increased viscosity may lead to reduced rates of oxygen transfer into the liquid phase in some systems. High polymers are also known to reduce drag, and therefore agitator power consumption, in flow systems even at concentrations too low to affect viscosity. This leads directly to a reduction in ε, further increasing eddy size. A beneficial effect of polymer addition on free-living human lymphoblastoid cells has been reported [45], although the effect was hypothesized to be mechanical protection of the cells by adsorbed polymer and possibly related to surface tension.

Raising the viscosity will also somewhat reduce microcarrier collisions against the impeller by increasing the drag force on the beads and reducing their tendency to deviate from the fluid streamlines. The effect is not large but it is present.

The size of the microcarrier beads should be optimized for each application. In systems where impeller collision is the primary source of damage, smaller beads have a lower collision frequency and a lower kinetic energy of collision. If bead-bead collision in turbulent eddies is the major damage mechanism, decreasing bead size lowers the collision energy but raises the frequency. Depending on which factor is more important, the optimal bead size may be either smaller or larger. Although smaller beads may reduce cell damage, they have the disadvantages of requiring the cells to adhere to a more curved surface, and of being more difficult to separate from the medium by either settling or filtration.

Collision damage can be minimized by rational impeller design. The smallest impeller, in terms of both diameter and number of blades, that gives adequate mixing should be used. Reducing impeller diameter has three advantages: it shrinks the impeller collision window; it reduces the relative speed of the microcarriers and the impeller, hence the energy of collision; and, as discussed in connection with bead-bead collisions caused by turbulence, it increases the scale of the smallest turbulence. Streamlining the blade cross-section, and in particular rounding the leading edge, will reduce the number of collisions. As noted already, polishing any rough surfaces and applying an elastic coating would mitigate the effects of any collisions that do occur.

Recalling that mixing is needed primarily to prevent relatively stagnant zones from forming, it is desirable to establish a large scale circulation without extremes of velocity. This could be accomplished and impeller collision eliminated by using externally recirculated liquid for mixing rather than using an agitator. Medium could be drawn off from the reactor and returned to it at locations that would ensure an adequate flow through all parts of the vessel. While outside the vessel this stream could be processed to replenish oxygen and nutrients or to remove product molecules. The turbulence around the return jets must be considered, but could be controlled by limiting the jet velocity. The biggest problem is likely to be developing an effective way of separating the microcarriers from a relatively large flow of culture medium so they would not be damaged in the circulation pump.

Alternatively, it is possible to utilize secondary flows generated by a very low speed agitator to provide reactor mixing [46], although this may not be sufficient as reactor size increases. This may be the operating principle behind the successful use of soft spiral vanes for agitation [2].

7 Conclusions

By analyzing the phenomena involved in agitation of microcarrier suspensions, harmful effects on cell cultures that have been attributed to "shear" are found to be better explained as effects of turbulence or collision. Changes meant to reduce shear have also reduced turbulence and collision, leading to improvements in the practice of cell culture. Other new approaches to reducing turbulence and collision are proposed. Studies to deter-

mine the response of cells to intermittent cyclic shear stress at frequencies in the range 5 to 30 Hz are suggested.

The analysis presented here allows the design of experiments to investigate and quantitate the effect of each possible mechanism of cell damage. This is accomplished by designing and operating the bioreactor so that the effect of a proposed or suspected mechanism is especially amplified. Work in this direction is currently in progress in our laboratory.

Acknowledgement

This study was performed under NASA grant NAS 9-17403 through the University of Texas Health Sciences Center (Houston).

References

1. Glacken, M. W.; Fleischaker, R. J.; Sinskey, A. J.: Mammalian cell culture: Engineering principles and scale-up. Trends Biotech. 1 (1983) 102–108
2. Feder, J.; Tolbert, W. R.: The large scale culture of mammalian cells. Sci. Am. 248 (1983) 36–43
3. Margaritis, A.; Wallace, J. B.: Novel bioreactor systems and their applications. Biotechnol. 2 (1984) 447–453
4. Midler, M., Jr.; Finn, R. K.: A model system for evaluating shear in the design of stirred fermentors. Biotechnol. Bioeng. 8 (1966) 71–84
5. Hirtenstein, M.; Clark, J.: In: Richards, R.; Rajan, K. (Eds.): Tissue culture in medical research. Oxford: Pergamon Press (1980)
6. Sinskey, A. J.; Fleischaker, R. J.; Tyo, M. A.; Giard, D. J.; Wang, D. I. C.: Production of cell-derived products: Virus and interferon. Ann. NY Acad. Sci. 369 (1981) 47–59
7. Croughan, M. S.; Wang, D. I. C.; Hamel, J.-F.: Fluid shear effects on animal cells grown in microcarrier cultures. Presented at AIChE National Meeting, Chicago, November 1985
8. Stathopoulos, N. A.; Hellums, J. D.: Shear stress effects on human embryonic kidney cells in vitro. Biotechnol. Bioeng. 27 (1985) 1021–1026
9. Frangos, J. A.; Eskin, S. G.; McIntire, L. V.; Ives, C. L.: Flow effects on prostacyclin production by cultured human endothelial cells. Sci. 227 (1985) 1477–1479
10. Fleischaker, R. J., Jr.; Sinskey, A. J.: Oxygen demand and supply in cell culture. Eur. J. Appl. Microbiol. 12 (1981) 193–197
11. Bird, R. B.; Stewart, W. E.; Lightfoot, E. N.: Transport phenomena, pp. 56–60. NY: Wiley & Sons 1960
12. Cooney, C. L.; Koplov, H. M.; Haggstrom, M.: Transient phenomena in continuous culture. In: Calcott, P. H. (Ed.): Continuous culture of cells. Florida: CRC Press, Boca Raton 1981
13. Harrison, D. E. F.; Topiwala, H. H.: Transient and oscillatory states of continuous culture. Adv. Biochem. Eng. 3 (1974) 167–220
14. Hansford, G. S.; Humphrey, A. E.: Effect of equipment scale and degree of mixing on continuous fermentation yield at low dilution rates. Biotechnol. Bioeng. 8 (1966) 85–96
15. Kolmogorov, D. N.; C. R. (Doklady) Acad. Sci. U.S.S.R., N.S. 30 (1941) 301–305
16. Hinze, J. O.: Turbulent fluid and particle interaction. Prog. Heat Mass Transfer 6 (1971) 433–452
17. Friedlander, S. K.: Behavior of suspended particles in a turbulent fluid. AIChE J. 3 (1957) 381–385
18. Panchev, S.: Random functions and turbulence, pp. 144–152. New York: Pergamon Press 1971
19. Nagata, S.: Mixing – principles and applications, pp. 138–164. New York: Halsted Press 1975
20. Giard, D. J.; Loeb, D. H.; Thilly, W. G.; Wang, D. I. C.; Levine, D. W.: Human interferon production with diploid fibroblast cells grown on microcarriers. Biotechnol. Bioeng. 21 (1979) 433–442
21. Soo, S. L.: Fluid dynamics of multiphase systems, p. 263. Mass.: Blaisdell Publ. Co., Waltham 1967
22. Lee, S. L.; Durst, F.: On the motion of particles in turbulent duct flows. Int. J. Multiphase Flow 8 (1982) 125–146
23. Microcarrier cell culture – principles and methods. Uppsala, Sweden: Pharmacia Fine Chemicals AB 1981
24. Einav, S.; Lee, S. L.: Particles migration in laminar boundary layer flow. Int. J. Multiphase Flow 1 (1973) 73–88
25. Nagata, S., op. cit., p. 36
26. Perry, R. H.; Chilton, C. H. (Eds.): Chemical engineers' handbook, 5th ed., p. 3–247. New York: McGraw-Hill 1973
27. Sather, N. F.; Lee, K. J.: Viscosity of concentrated suspensions of spheres. Prog. Heat Mass Trans. 6 (1972) 575–589
28. Placek, J.; Tavlarides, L. L.: Turbulent flow in stirred tanks. Part I: Turbulent flow in the impeller region. AIChE J. 31 (1985) 1113–1120
29. Schlichting, H.: Boundary layer theory, 7th ed., pp. 636–640. New York: McGraw-Hill 1979
30. Ibid, pp. 695–696
31. Ibid, pp. 135–144
32. Brenner, H.: Particles in low Reynolds number flows. Prog. Heat Mass Transfer 6 (1971) 509–574
33. Saffman, P. G.: The lift on a small sphere in slow shear flow. J. Fluid Mech. 22 (1965) 385–400
34. Immich, H.: Impulsive motion of a suspension: Effect of antisymmetric stresses and particle rotation. Int. J. Multiphase Flow 6 (1980) 441–471
35. Cox, R. G.; Zia, I. Y. Z.; Mason, S. G.: Particle motions in sheared suspensions: XXV. Streamline around cylinders and spheres. J. Colloid Interface Sci. 27 (1968) 7–18
36. Adamczyk, Z.; van de Ven, T. G. M.: Pathlines around freely rotating spheroids in simple shear flow. Int. J. Multiphase Flow 9 (1983) 203–217
37. Goldman, A. J.; Cox, R. G.; Brenner, H.: Slow viscous motion of a sphere parallel to a plane wall-II. Couette flow. Chem. Eng. Sci. 22 (1967) 653–660
38. Eichhorn, R.; Small, S.: Experiments on the lift and drag of spheres suspended in a Poiseuille flow. J. Fluid Mech. 20 (1964) 513–527
39. Spielman, L. A.: Particle capture from low-speed laminar flows. Ann. Rev. Fluid Mech. 9 (1977) 297–319
40. Davies, C. N.: Air filtration, chap. 3. New York: Academic Press 1973
41. Schlichting, H., op. cit., p. 39
42. Bird, R. B. et al., op. cit., p. 136
43. Schlichting, H., op. cit., p. 97–98
44. Nagata, S., op. cit., p. 10
45. Mizrahi, A.: Oxygen in human lymphoblastoid cell line cultures and effect of polymers in agitated and aerated cultures. Dev. Biol. Stds. 55 (1984) 93–102
46. De Bruyne, N. A.: A high efficiency stirrer for suspension cell culture with or without microcarriers. Adv. Exp. Med. Biol. 172 (1984) 139–149

Received November 8, 1985

R. S. Cherry
E. T. Papoutsakis
Department of Chemical Engineering
Rice University
P.O. Box 1892
Houston, Texas 77251-1892
USA